Université catholique de Louvain

LMECA2660 - Numerical Methods in Fluid Mechanics

Homework 1 - Simulating convection

Academic year 2022-2023

Otis Van Kerm : 35561900

1 Introduction

For this homework, we would like to simulate the convection of a certain quantity u at constant speed c. This phenomenon follows the equation:

$$\frac{\partial u}{\partial t} + c\frac{\partial u}{\partial x} = 0 \tag{1}$$

By dividing equation (1) by $\frac{Uc}{L}$, with L being a representative length scale and U a constant with the same dimensions as u, we can rewrite the equation in an non-dimensional form:

$$\frac{\partial u'}{\partial t'} + \frac{\partial u'}{\partial x'} = 0 \tag{2}$$

with $u' = \frac{u}{U}$, $x' = \frac{x}{L}$ and $t' = \frac{ct}{L}$ the non-dimensional variables of our problem. Making the equation non-dimensional is equivalent to setting c, U and L to one and removing them from the equation. In the code, we will be solving this non-dimensional equation.

The function that we will use as initial condition is a Gaussian function defined as:

$$u(x, 0) = U \exp\left(-\frac{x^2}{\sigma^2}\right)$$

2 Discretized periodic domain

For the simulations, we restrict the domain from $\frac{-L}{2}$ to $\frac{L}{2}$, discretize the domain into a fixed number of points and make the domain periodic. Under these circumstances, any function can be decomposed into modes using the discrete Fourier transform. These coefficients will then give us the amplitude of each mode, the j^{th} Fourier coefficient will give the amplitude of the mode with wavenumber $k_j = \frac{2\pi j}{L}$. Here are plots of the discrete Fourier transform for the Gaussian function in this periodic domain and the Fourier transform of the Gaussian function in an unbounded domain:

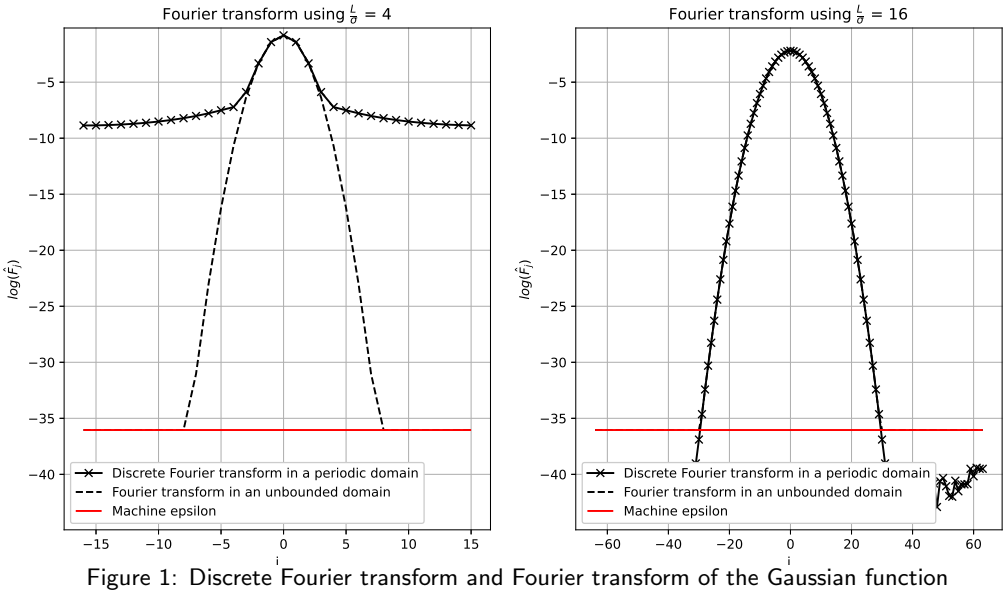

Figure 1: Discrete Fourier transform and Fourier transform of the Gaussian function

For ease of readability, the Fourier transform in an unbounded domain has been bounded from below with the machine epsilon.

For the case with $\frac{L}{\sigma} = 4$, for high j, the plots start to differ by a lot so the approximation in the discretized domain will not approximate the real Gaussian correctly. The modes with high wavenumbers will be stronger than they should be.

For the case with $\frac{L}{\sigma} = 16$, we can see that the graphs are very similar. This means that the approximate solution has the same frequency content as the real solution. We can then assume that the approximate solution is very close to the real solution. In all of the simulations we will then use $\frac{L}{\sigma} = 16$.

3 Partially decentered scheme

3.1 Equation for the ED scheme

We will first write out the Taylor series for u_{i-2}, u_{i-1} and u_{i+1} around $x = x_i$, where $u_i = u(x_i)$:

$$u_{i+1} = u_i + h \left.\frac{\partial u}{\partial x}\right|_i + \frac{h^2}{2} \left.\frac{\partial^2 u}{\partial x^2}\right|_i + \frac{h^3}{6} \left.\frac{\partial^3 u}{\partial x^3}\right|_i + \frac{h^4}{24} \left.\frac{\partial^4 u}{\partial x^4}\right|_i + \mathcal{O}(h^5)$$
$$u_{i-1} = u_i - h \left.\frac{\partial u}{\partial x}\right|_i + \frac{h^2}{2} \left.\frac{\partial^2 u}{\partial x^2}\right|_i - \frac{h^3}{6} \left.\frac{\partial^3 u}{\partial x^3}\right|_i + \frac{h^4}{24} \left.\frac{\partial^4 u}{\partial x^4}\right|_i + \mathcal{O}(h^5)$$
$$u_{i-2} = u_i - 2h \left.\frac{\partial u}{\partial x}\right|_i + 2h^2 \left.\frac{\partial^2 u}{\partial x^2}\right|_i - \frac{4h^3}{3} \left.\frac{\partial^3 u}{\partial x^3}\right|_i + \frac{2h^4}{3} \left.\frac{\partial^4 u}{\partial x^4}\right|_i + \mathcal{O}(h^5)$$

where $|_i$ means "evaluated at point x_i".

We can do a linear combination of these 3 expressions to get:

$$\begin{aligned} &a\, u_{i-2} + b\, u_{i-1} + c\, u_{i+1} \\ &= (a+b+c)u_i + h(-2a-b+c) \left.\frac{\partial u}{\partial x}\right|_i + h^2(2a + \frac{b}{2} + \frac{c}{2}) \left.\frac{\partial^2 u}{\partial x^2}\right|_i \\ &+ h^3(\frac{-4a}{3} - \frac{b}{6} + \frac{c}{6}) \left.\frac{\partial^3 u}{\partial x^3}\right|_i + h^4(\frac{2a}{3} + \frac{b}{24} + \frac{c}{24}) \left.\frac{\partial^4 u}{\partial x^4}\right|_i + \mathcal{O}(h^5) \end{aligned}$$

With this, we can eliminate the terms including $\left.\frac{\partial^2 u}{\partial x^2}\right|_i$ and $\left.\frac{\partial^3 u}{\partial x^3}\right|_i$. We cannot eliminate the term with $\left.\frac{\partial^4 u}{\partial x^4}\right|_i$ because this would give $a = b = c = 0$ which is not useful for us as it also eliminates the $\left.\frac{\partial u}{\partial x}\right|_i$ that is of interest. We then have:

$$\begin{cases} 4a + b + c = 0 \\ -8a - b + c = 0 \end{cases}$$

Which gives $b = -6a$ and $c = 2a$. Re injecting this into the equation above gives:

$$a\, u_{i-2} - 6a\, u_{i-1} + 2a\, u_{i+1} = -3a\, u_i + h\, 6a \left.\frac{\partial u}{\partial x}\right|_i + h^4 \frac{a}{2} \left.\frac{\partial^4 u}{\partial x^4}\right|_i + \mathcal{O}(h^5)$$

By isolating $\left.\frac{\partial u}{\partial x}\right|_i$, we get:

$$\left.\frac{\partial u}{\partial x}\right|_i = \frac{1}{6h}(u_{i-2} - 6u_{i-1} + 3u_i + 2u_{i+1}) - \frac{h^3}{12} \left.\frac{\partial^4 u}{\partial x^4}\right|_i + \mathcal{O}(h^4) \tag{3}$$

The equation for the ED scheme will then be:

$$\left.\frac{\partial u}{\partial x}\right|_i \approx \frac{1}{6h}(u_{i-2} - 6u_{i-1} + 3u_i + 2u_{i+1}) \tag{4}$$

3.2 Order and truncation error

By inspection of the formula for the ED scheme (3), we can see that our method is of order 3 and the truncation error is $\frac{h^3}{12} \left.\frac{\partial^4 u}{\partial x^4}\right|_i$.

3.3 Modified wave number

We can rewrite equation (1) as:

$$\frac{\partial u}{\partial t} = -c\frac{\partial u}{\partial x} \tag{5}$$

If we assume a solution of the shape $u(t) = \sum_j \hat{U}_j(t)e^{ik_j x}$, we can analyse the behaviour of only one mode because our PDE is linear. Replacing one of the modes into (5) gives us:

$$\frac{d\hat{U}_j}{dt} = -cik_j\hat{U}_j \tag{6}$$

$$= \lambda_j\hat{U}_j \tag{7}$$

Which is the exact solution. If we now use our ED scheme (4) for the x derivative $\frac{\partial u}{\partial x}$, we can get by evaluating (5) at point x_i that:

$$\begin{aligned}
\frac{d\hat{U}_j}{dt}e^{ik_j x_i} &= \frac{-c}{6h}\left(e^{ik_j x_{i-2}} - 6e^{ik_j x_{i-1}} + 3e^{ik_j x_i} + 2e^{ik_j x_{i+1}}\right)\hat{U}_j \\
&= \frac{-c}{6h}\left(e^{ik_j x_i}e^{-2ik_j h} - 6e^{ik_j x_i}e^{-ik_j h} + 3e^{ik_j x_i} + 2e^{ik_j x_i}e^{ik_j h}\right)\hat{U}_j \\
\frac{d\hat{U}_j}{dt} &= \frac{-c}{6h}\left(e^{-2ik_j h} - 6e^{-ik_j h} + 3 + 2e^{ik_j h}\right)\hat{U}_j \\
\Rightarrow \lambda_j^* &= \frac{-c}{6h}\left(e^{-2ik_j h} - 6e^{-ik_j h} + 3 + 2e^{ik_j h}\right) \\
\Rightarrow k_j^* h &= \frac{\lambda_j^* h}{-ic} \\
&= \frac{-i}{6}\left(e^{-2ik_j h} - 6e^{-ik_j h} + 3 + 2e^{ik_j h}\right)
\end{aligned}$$

3.4 Error on the actual wave number

Using the equation for k^*h, we can see that it is a complex number and we can then write it as $k^*h = k_r h + ik_i h$. In the case of the exact solution, we should have $k_r = k$ and $k_i = 0$. This will not be the case here, we can plot $k_r h$ and $k_i h$ in terms of kh:

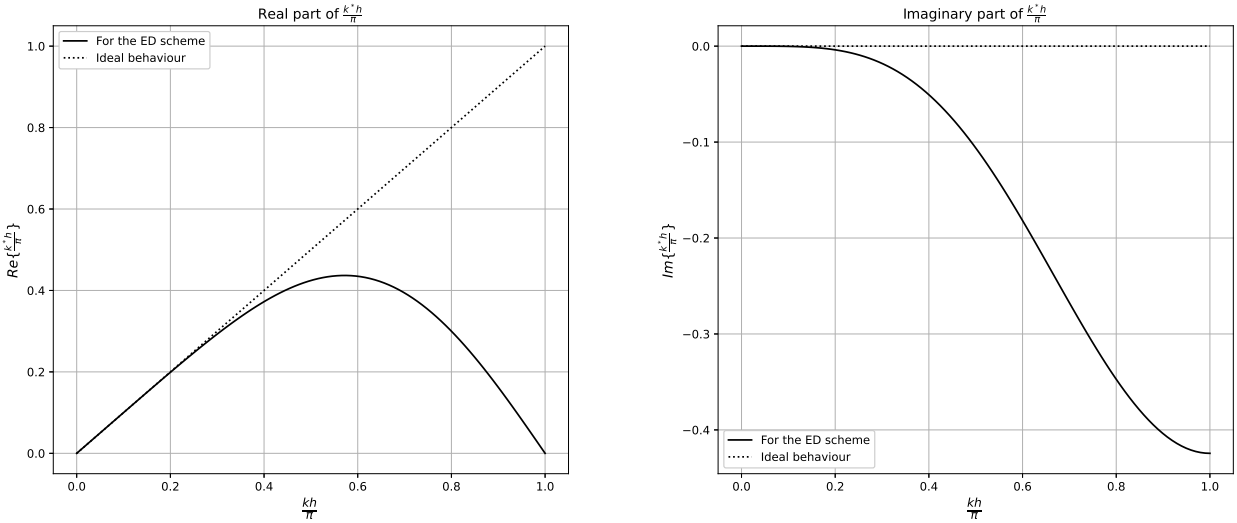

(a) Real part of the modified wave number (k_r) (b) Imaginary part of the modified wave number (k_i)

Figure 2: Components of the modified wave number

If we insert this modified wavenumber into equation (6) and solve for $\hat{U}$, we find:

$$\hat{U}(t) = \hat{U}(0)e^{-ic(k_{j,r}h + ik_{j,i}h)t} \tag{8}$$

$$= \hat{U}(0)e^{-ick_{j,r}ht}e^{k_{j,i}ht} \tag{9}$$

We then see that $k_{j,r}h$ is related to the speed at which the mode j is convected. The closer $k_{j,r}h$ is to kh, the closer the speed at which this mode is convected will be to c. We can then see from figure 2a that for small wave numbers, the ED scheme will do convection at the correct speed. On the other hand, the modes with the highest wavenumbers will not even be convected since $k_{j,r}h$ tends to 0.

In the case where $k_{j,i}h$ is less than 0, like we have for the ED scheme, equation (9) tells us that the amplitude of the mode j will decrease exponentially with a rate $k_{j,i}h$. We can see from figure 2b that $k_{j,i}h$ decreases with kh so the amplitude of the modes with high wavenumbers will decrease faster than those with low wavenumbers. This ED scheme will then cause some diffusion on top of the advection.

4 Stability

For the approximation of $\frac{du}{dx}$, we will be using four different schemes named E2, E4, ED and I4. E2 and E4 are centered schemes of orders 2 and 4 while I4 is an implicit method of order 4. ED is the partially decentered scheme described in section 3.

For each of these methods, we can compute the modified wavenumber and so the value of k^*h. By defining the CFL number as $CFL = \frac{c\Delta t}{h}$ and λ^* defined like in section 3, we have $\lambda^*\Delta t = -i \cdot CFL \cdot k^*h$. For these schemes to be stable when using a Runge-Kutta 4 scheme for the time integration, we need to have, for all k^*h, that:

$$\rho = 1 + (\lambda^*\Delta t) + \frac{1}{2}(\lambda^*\Delta t)^2 + \frac{1}{6}(\lambda^*\Delta t)^3 + \frac{1}{24}(\lambda^*\Delta t)^4 < 1$$

Using this equation, we can then find the maximum CFL number that we can use for each scheme. Here are the results:

Scheme	E2	E4	ED	I4
CFL_{max}	2.828	2.061	1.744	1.631

If we want to use the same CFL number for each scheme, we should use a CFL number less than 1.631. However, the smaller the CFL number, the closer we are to $\rho = 1$ so we have a high precision. Considering this, we will use a $CFL = 0.5$ for the simulations and we can then look at how each scheme fits into the RK4 curve:

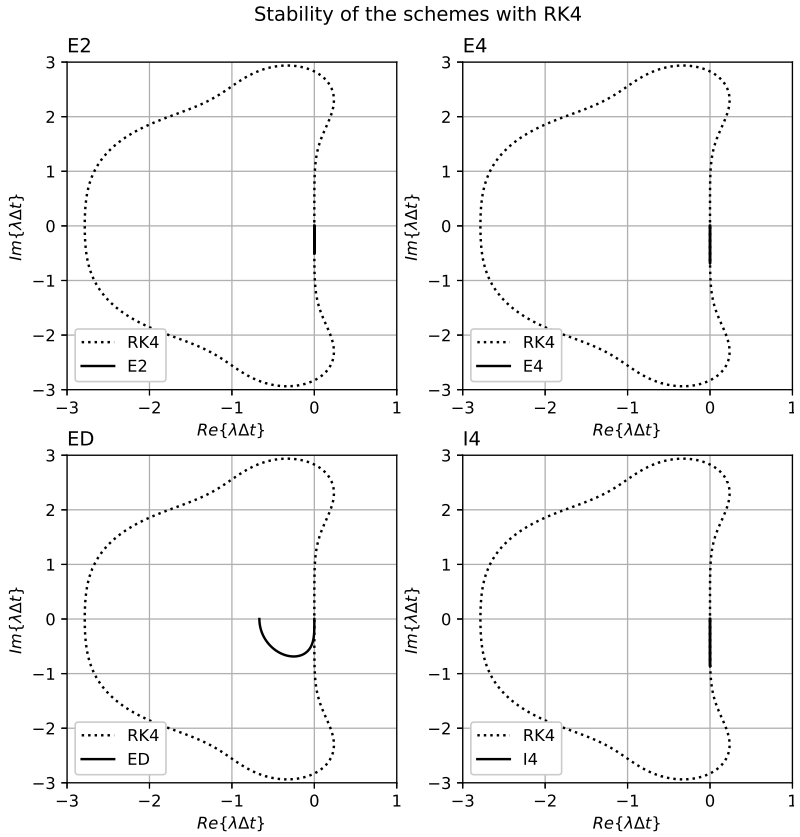

Figure 3: Fit of each scheme inside of the RK4 curve

We see that except for the ED scheme, we are very close to $\rho = 1$ so our results will be accurate. In the case of the ED scheme, we are going away from the imaginary axis and into the numbers with a real part that is negative. This means that this scheme is diffusive and induces a numerical diffusion in the solution.

5 Implementation

As said before, an adimentionalised version of the convection is implemented, see equation (2). In the code, e are using a structure with every details of the simulation like the number of points N, the value of h and σ, ... We are also defining inside of the structure the scheme that we want to use for approximating $\frac{du}{dx}$. This structure will change at each time step, containing the values of u at time t. During the initialisation of the problem, we can choose whether to use a non uniform grid or not or whether we want to use a wave packet for the initial condition (see later). Time integration is done with a Runge-Kutta 4 scheme and results are saved in text files. How to use this code is explained in the README in the files attached.

6 Analysis of the results

6.1 Comparison of the numerical and analytical solutions

Using the code, we can simulate the advection of a Gaussian function using each scheme and either 32, 64 or 128 points. Here are the results of the these simulations:

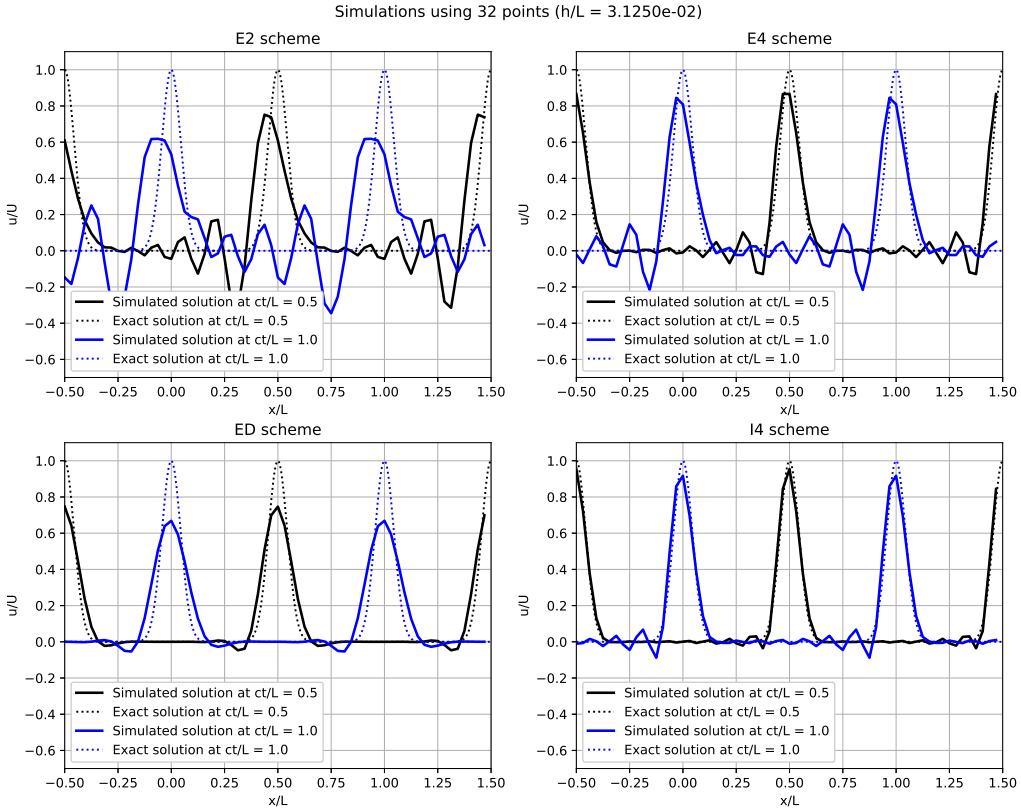

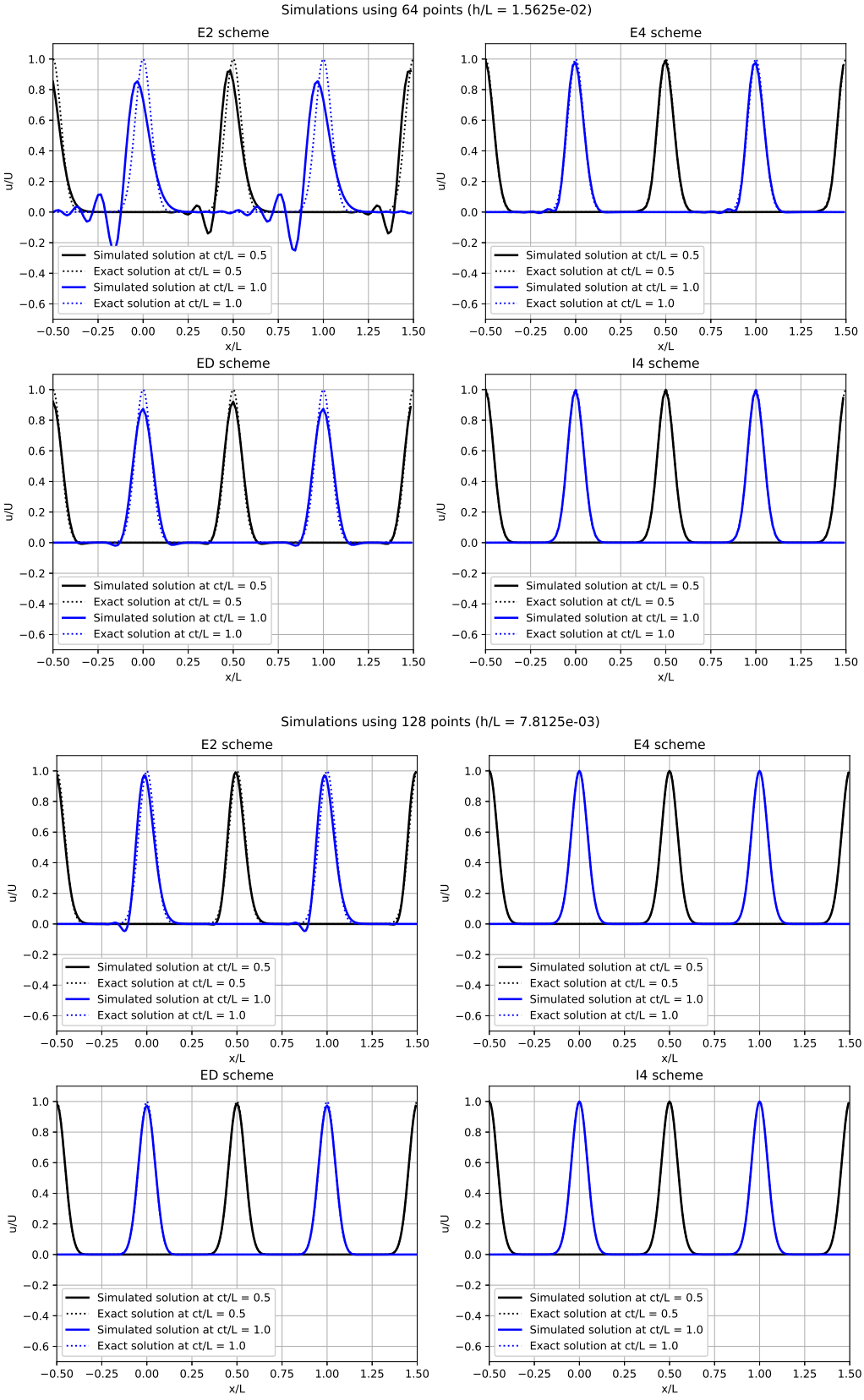

Figure 4: Simulated solutions and analytical solutions for the 4 schemes and two different adimentional times

We'll firstly do a qualitative analysis of these plots and then a qualitative analysis of the results is done in the next section. We can see that the simulated solutions are further from the real solution as the number of points is small. Increasing the number of points gives then much better results. By looking at the plots of the E2, E4 and I4 schemes for 64 points, we can see that the I4 scheme is the best performing of all of these then the E4 and finally the E2 scheme. Furthermore, for each of these schemes we can see spurious oscillations downstream of the bump (to the left). Looking at the solutions for the ED scheme with 32 points, we can see that the bumps are a lot smaller and wider for the simulation than the real solution. These are the effects of diffusion, which we should expect from this scheme. However, this schemes seems to better keep the symmetry of the Gaussian function.

6.2 Evolution of the global diagnostics

At each time step of the simulation, we have computed three global diagnostics that can help us understand the effects of each schemes on the simulation. The first one is $I^n = (h\sum_i u_i^n)/(\sigma U)$, it approximates the integral under the curve. In the case of a Gaussian function, this integral should be equal to $\sqrt{\pi} \approx 1.772$. The second one is $E^n = (h\sum_i (u_i^n)^2)/(\sigma U^2)$, it approximates the integral of the square of the function, it is then related to the energy present in the signal. Simple advection should keep this value constant while diffusion will decrease it. The third one is $R^n = (h\sum_i (u_i^n - u(x_i, t^n))^2)/(\sigma U^2)$, it measures the square of the error between the simulation and the analytical solution at each time step. Here is how each diagnostics evolves with time depending on the integration scheme and the number of grid points:

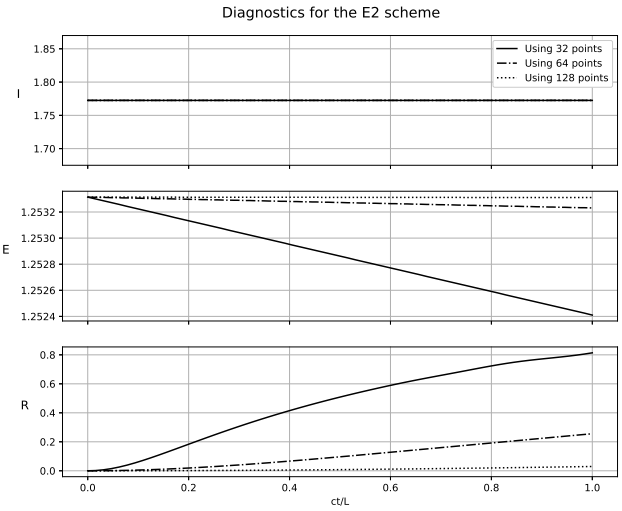

(a) E2 scheme

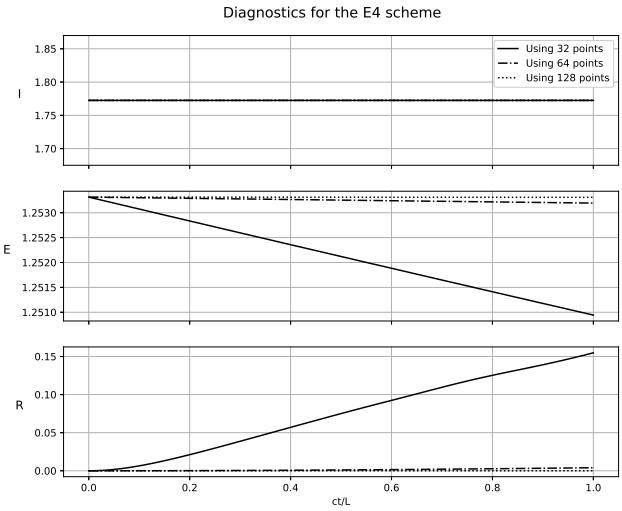

(b) E4 scheme

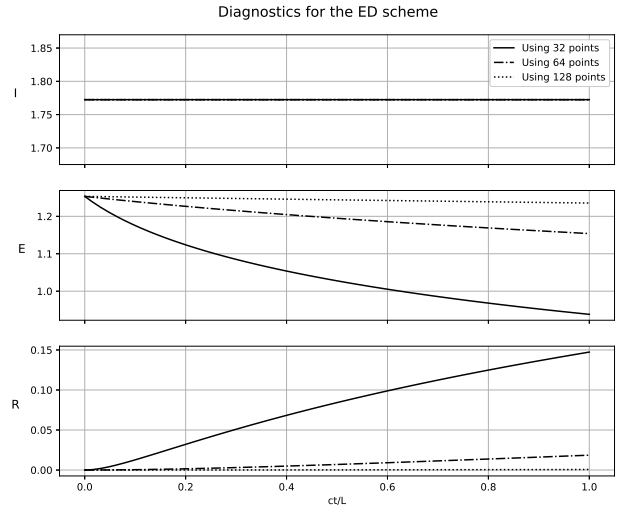

(c) ED scheme

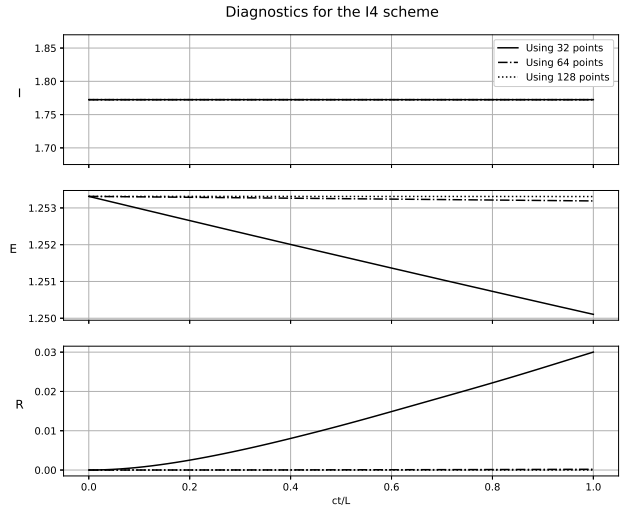

(d) I4 scheme

Figure 5: Evolution of the global diagnostics for each scheme

From these graphs, we can see that each scheme keeps the I diagnostic, the approximate integral of the function, constant. This is a good property as it means that no material is added to the function. For example, if we are convecting a mass density ρ, the total mass, which is the integral of ρ, stays constant so no mass is added.

By looking at the E diagnostic, we can see that each scheme induces a bit of diffusion and decreases the value of E. We can compute the relative difference in E between the times $\frac{ct}{L} = 0$ and $\frac{ct}{L} = 1$ for 32 points to get:

Scheme	E2	E4	ED	I4
Relative difference in E	0.07%	0.18%	24.20%	0.26%

It is clear from the table that the ED scheme induces a lot more diffusion than all of the other schemes, which is to be expected as is explained in section 3.4. From figure 3, we can see that the I4 scheme goes lower down in the negative imaginary numbers that the E2 scheme. This means the average value of the amplification factor ρ of the RK4 method will be lower and further from 1 for the I4 scheme rather than for the E2 scheme. The RK4 method will then induce more diffusion when used with the I4 scheme rather than with the E2 scheme, which is what we observe on the above

graphs. For each of the schemes, we can see that the more points we have, the lower is the amount of lost energy.

Looking at the R diagnostic allows us to see that the I4 scheme gives the smallest error and that the E2 scheme gives the highest error. We also observe that as the number of points increases, the error gets smaller. Using this diagnostic, we will be able to calculate the order of convergence of each scheme, this is done in the next section.

6.3 Order of convergence of the different numerical methods used

We can run the simulations for different values of $\frac{h}{\sigma}$ and calculate the R diagnostics at time $\frac{ct}{L} = 0.5$ for each of the schemes. Here are the results plotted in a log-log plot for $\frac{h}{\sigma} = \frac{1}{2^k}$, for $k \in \{1, 2, ..., 7\}$:

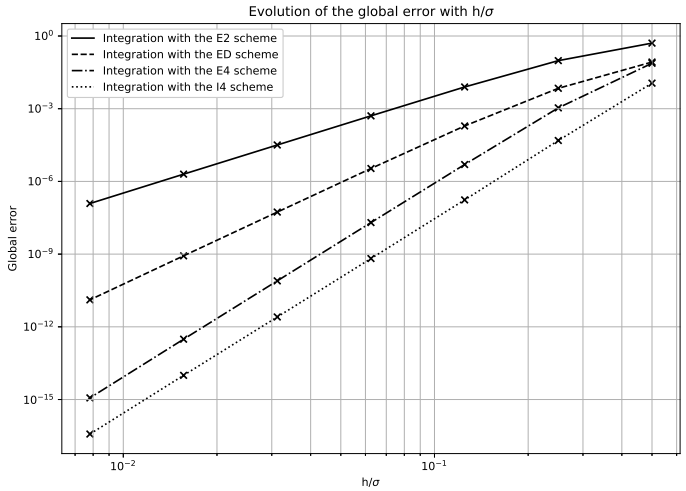

Figure 6: Global error of each scheme at time $\frac{ct}{L} = \frac{1}{2}$ and for different $\frac{h}{\sigma}$

For small values of $\frac{h}{\sigma}$, we can see that graphs are linear, which means that asymptotically, we have an error that is of order $\mathcal{O}(h^\alpha)$. In order to find alpha, we need to find the slopes of these lines in the log-log plot and the order of the corresponding scheme will be the value of the slope halved. This division by 2 is explained because we are plotting the R diagnostic, which is the square of the error so a factor of 2 appears by taking the logarithm. Using this, we can find:

Scheme	E2	ED	E4	I4
Slope in the log-log plot	4.01	6.01	8.02	8.02
Estimated order of convergence	2	3	4	4

This is in line with the results that we obtained in the lecture notes and in section 3.2.

7 Non uniform grid spacing

7.1 Convection equation in the numerical space

We have a mapping from the numerical space ξ to the physical space x so we can write $x = g(\xi)$. We would then like to rewrite the convection equation in the numerical space so in the form:

$$\frac{\partial v}{\partial t} + \frac{\partial (bv)}{\partial \xi} = 0$$

Using the chain rule, we can rewrite $\frac{\partial u}{\partial x}$:

$$\frac{\partial u}{\partial x} = \frac{d\xi}{dx}\frac{\partial u}{\partial \xi} = \frac{1}{\frac{dx}{d\xi}(\xi)}\frac{\partial u}{\partial \xi}$$

Inserting this into the convection equation gives:

$$\begin{aligned}
\frac{\partial u}{\partial t} + \frac{c}{\frac{dx}{d\xi}}\frac{\partial u}{\partial \xi} &= 0 \\
\frac{dx}{d\xi}\frac{\partial u}{\partial t} + c\frac{\partial u}{\partial \xi} &= 0 \qquad (\frac{dx}{d\xi} \text{ is not zero, see later}) \\
\frac{\partial}{\partial t}\left(\frac{dx}{d\xi}u\right) + \frac{\partial}{\partial \xi}(cu) &= 0 \qquad (\frac{dx}{d\xi} \text{ does not depend on time and } c \text{ is constant}) \\
\frac{\partial v}{\partial t} + \frac{\partial}{\partial \xi}\left(\frac{c}{\frac{dx}{d\xi}}v\right) &= 0 \qquad (\text{by setting } v = \frac{dx}{d\xi}u)
\end{aligned}$$

From the last equation, we can see that the convection equation inside the numerical space can be written in the conservative form $\frac{\partial v}{\partial t} + \frac{\partial (bv)}{\partial \xi} = 0$ with $b(\xi) = \frac{c}{\frac{dx}{d\xi}}$ and $v(\xi, t) = \frac{dx}{d\xi}u$. As before, dividing this equation by $\frac{Uc}{L}$ allows us to make it adimentional, which is equivalent to setting $c = 1$.

In our case, the mapping that we will use is:

$$x = g(\xi) = \xi - a\frac{L}{2\pi}\sin\left(2\pi\frac{\xi}{L}\right)$$

Taking the derivative gives:

$$\frac{dx}{d\xi} = g'(\xi) = 1 - a\cos\left(2\pi\frac{\xi}{L}\right)$$

In our simulations, we used $a = \frac{3}{5}$, we can then see that we indeed have $\frac{dx}{d\xi} > 0$. Te calculations done above are then correct. The finest resolutions in physical space is around $x = 0$ and the coarsest are around $x = \pm\frac{L}{2}$.

7.2 Results

Using this, we can simulate the convection of the Gaussian function using each integration scheme described in section 4. Here are the results of our functions in numerical space, $\frac{v(\frac{\xi}{L})}{U}$, and in physical space, $\frac{u(\frac{x}{L})}{U}$:

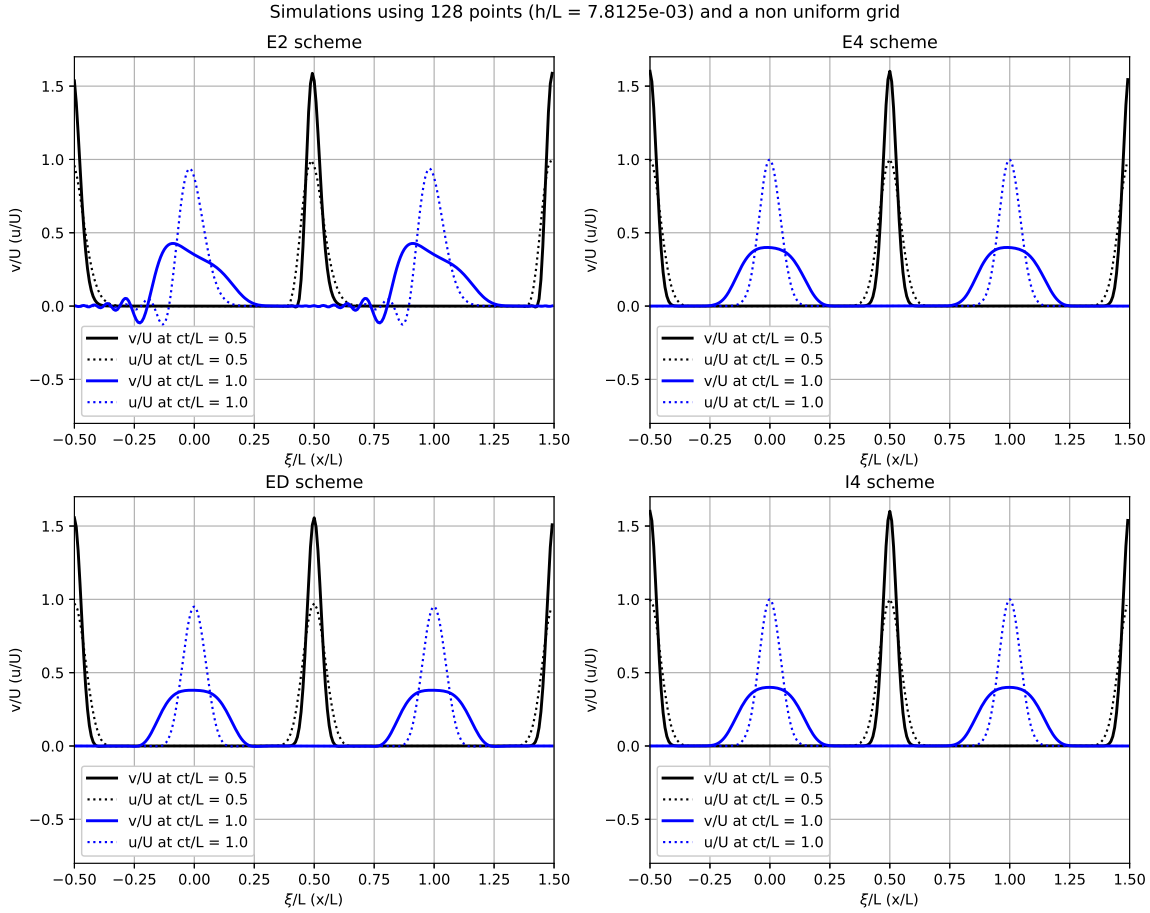

Figure 7: Convection using a non uniform grid

As expected, like all of the above simulations, the E2 scheme is the worst performing of all of these and we can see oscillations appearing on the left side of the bump. By comparing the solution $\frac{u(\frac{x}{L})}{U}$, in the dotted lines above, with the solution found for a uniform grid 4, we can see that there is more diffusion for the ED scheme when using a non uniform grid.

The relationship between u and v is given by $v = \frac{dx}{d\xi}u$. For $x \approx 0$ we have $\xi \approx 0$ so $\frac{dx}{d\xi} \approx 1 - a = \frac{2}{5}$ so around $x = 0$ we should have $v \approx 0.4u$. We can see on the graphs above that this is indeed the relationship that we have. On the sides of the domain, for $x \approx \pm\frac{L}{2}$ so $\xi \approx \pm\frac{L}{2}$, we have $\frac{dx}{d\xi} \approx 1 + a = \frac{8}{5}$. So at the boundaries, we should have $v \approx 1.6u$ which is again the behaviour that we observe on the above graphs.

8 Convection of a wave packet

By changing the initial condition from a Gaussian function to a wave packet, we can test our code with a function that has modes of higher wavenumbers. Here is the initial condition that we used:

$$u(x,0) = U\cos(k_p x)\exp(-\frac{x^2}{\sigma^2}) \tag{10}$$

with $p = 8$ so $k_p = 16\pi$.

By taking the Fourier transform of equation (10), we can see which modes ar present in this function:

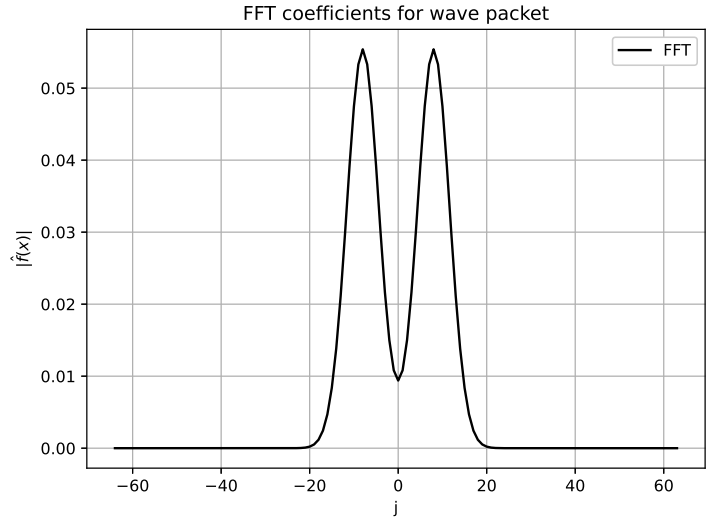

Figure 8: Fourier transform of the wave packet

From this graph, we can see that the prevalent modes are the ones from $j = 0$ to $j = 20$. Because we are using 128 points for this simulation, it means that these correspond to modes with $k_j h$ ranging from 0 to 0.3125.

For each of the schemes, we can define the group velocity, which is the speed at which each mode will be convected. It is defined as:

$$c_g^* = \frac{dk^*}{dk} c$$

Here is a graph of this group velocity in terms of j, note that we only keep the real part as the imaginary part causes diffusion and not convection:

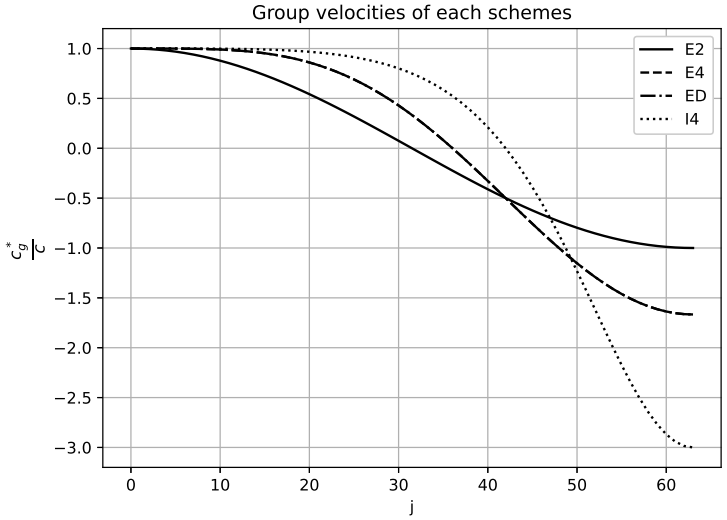

Figure 9: Real part of the group velocities of each scheme

For the wave packet that we used, we have c_j^* that is positive for every wavenumber and every scheme. This means that all of the wavenumbers will propagate to the right and not propagate downstream which would be unphysical. We can also see on this graph that the E4 and ED schemes have the same graph for c_g^*.

Here is a graph of the simulated and analytical solutions for two adimensional times and using each of the four schemes:

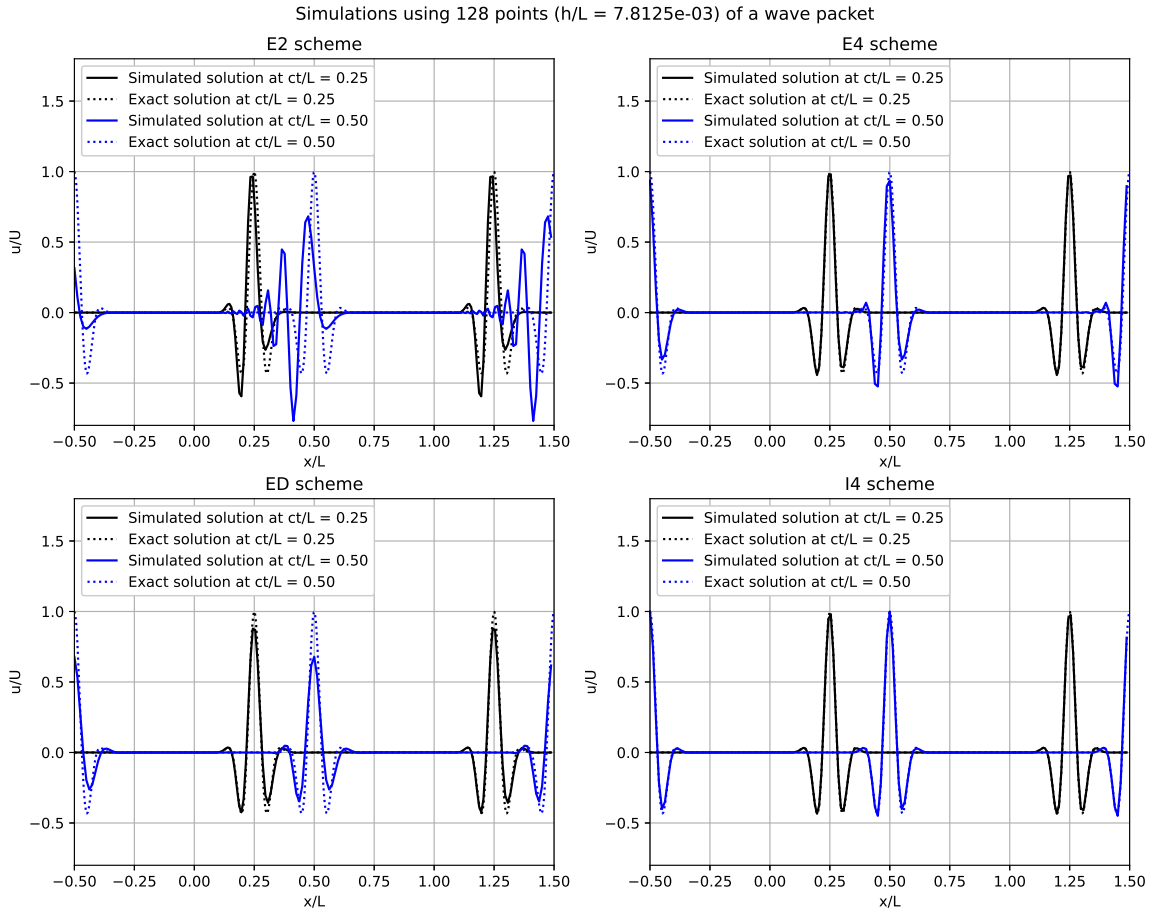

Figure 10: Convection of a wave packet using a non uniform grid

As before, we see some spurious oscillations to the left of the wave packet when using the E2 scheme. This can be explained using the graph in figure 9. We can see that higher wavenumbers travel slower than the velocity c so the high frequency oscillations in our signal will appear downstream of the other lower frequency signals that compose the wave packet. We again see diffusion when using the ED scheme and the I4 scheme is the one that gives the best results. This can also be explained using figure 9, for j ranging from 0 to 20, c_g^* is very close to c so the convection is done at the correct speed. We can also note that the simulations using the ED and E4 schemes seem to be the same up to a vertical stretching. It is in line with what we have observed before as we saw that they both have the same group velocity but the ED scheme also has a diffusion term that is added.